Parallel cortical-brainstem pathways to attentional analgesia

Valeria Oliva[1], Rob Gregory[1,2], Wendy-Elizabeth Davies[1,2], Lee Harrison[3], Rosalyn Moran[4], Anthony E. Pickering[1,2], Jonathan C.W. Brooks[3].

1 School of Physiology, Pharmacology & Neuroscience, Biomedical Sciences Building, University of Bristol, Bristol, BS8 1TD.

2 Anaesthesia, Pain & Critical Care Sciences, Bristol Medical School, University Hospitals Bristol, Bristol, BS2 8HW.

3 School of Psychological Science, University of Bristol, Bristol, BS8 1TU.

4 Department of Neuroimaging, Institute of Psychiatry, Psychology & Neuroscience, King's College London, SE5 8AF.

Abstract

Pain perception is diminished when attention is diverted. Our previous human fMRI study, using a 2x2 factorial design with thermal stimuli and concurrent visual attention task, linked the brainstem triad of locus coeruleus (LC), rostroventromedial medulla (RVM) and periaqueductal grey (PAG) to attentional analgesia. This study was repeated with a larger cohort, replicating our earlier findings. Pain intensity was encoded by the RVM, whilst activity in the contralateral LC correlated with the magnitude of attentional analgesia. Psycho-Physiological Interaction analysis informed subsequent Dynamic Causal Modelling and identified two parallel paths between forebrain and the brainstem regions involved in analgesia. These cortico-brainstem connections were modulated by attentional demand: a bidirectional anterior cingulate cortex (ACC) – right-LC loop, and a top-down influence of task on ACC-PAG-RVM. Under conditions of competing attentional demands the ACC recruits discrete brainstem circuits to modulate nociceptive input.

Introduction

Attentional analgesia is a well-characterised phenomenon whereby increased cognitive load can decrease pain perception (Peyron et al. 2000; Bantick et al. 2002; Brooks et al. 2002; Valet et al. 2004; Brooks et al. 2017; Sprenger et al. 2012). For example, this can be achieved by diverting attention from a painful stimulus to a visual task or simply by active mind-wandering (Bushnell et al., 2013; Kucyi et al., 2013). Central to attentional analgesia is the concept of divided attention, whereby less cognitive resource is available to be allocated to nociception and pain. Since noxious stimuli are inherently salient and therefore attention grabbing (Eccleston et al., 1999), then any concurrent cognitive task must compete for 'attentional' resource. Attention is thus cast both as a key component of pain behaviour (i.e. attending to pain (Crombez et al., 2004; Legrain et al., 2009; Roelofs et al., 2002)) as well as a putative mechanism for pain relief. The processes regulating attentional focus is of importance in the development, maintenance and potentially resolution of chronic pain states.

The mechanisms that allow attention to regulate pain are currently not well understood and there has been ongoing debate about whether attentional analgesia requires engagement of descending control to attenuate nociception (Brooks et al., 2017; Bushnell et al., 2013; Lorenz, Minoshima, & Casey, 2003; Tracey et al., 2002; Valet et al., 2004). Several important regions have been linked to the descending analgesic effects, including the anterior cingulate cortex (ACC), dorsolateral prefrontal cortex (dlPFC) and components of the descending pain control system including periaqueductal grey (PAG), rostroventromedial medulla (RVM) and locus coeruleus (LC). An interaction between cortical and mid-brain structures during distraction from pain has been identified (Lorenz et al., 2003; Valet et al., 2004) but these previous studies were unable to examine interactions in pontomedullary regions that are known to be important for the descending control of nociception.

These brainstem regions are all candidates for mediating attentional analgesia given their known anti-nociceptive roles (Millan, 2002). For example, multiple animal studies have demonstrated that

interactions between the PAG and RVM produces endogenous analgesia, mediated by spinally projecting neurons in the RVM (Basbaum et al., 1979; Fields et al., 1978; Heinricher et al., 2009). Together with the ACC, these regions form one of the main pain modulatory pathways involved in the bidirectional modulation (i.e. facilitation and inhibition) of nociception in the spinal cord dorsal horn (De Felice et al., 2016; Ossipov et al., 2010; Quintero, 2013).

Similarly, the LC is another potential candidate region that could mediate the interaction between attention and pain because of its projections to the spinal cord which release noradrenaline to produce analgesia (Hirschberg et al., 2017; Llorca-Torralba et al., 2016). Additionally, it has a known role in salience signalling and attention mediated by ascending projections (Aston-Jones et al., 1999; Sales et al., 2019; Sara et al., 2012). Despite it being challenging to resolve with fMRI (Astafiev et al., 2010; Liu et al., 2017), the LC was recently identified as the only region whose activity reflected the interaction between task and temperature in an attentional analgesia paradigm (Brooks et al., 2017). The LC could therefore contribute to attentional analgesia as part of the PAG-RVM system, or as a parallel descending modulatory pathway perhaps receiving inputs directly from ACC (Aston-Jones et al., 1991; Bajic et al., 1999).

Within this framework the ACC is ideally placed to mediate between competing cognitive demands (e.g. between a sustained visual attention task and pain) as it is active during conflict resolution (Braver et al., 2001; Kerns, 2006; Kim et al., 2011), its activity is modulated by attention (Davis et al., 2000) as well as being consistently activated by painful stimuli (Brooks et al., 2017; Garcia-Larrea et al., 2013; Peyron et al., 2000; Wager et al., 2013). The ACC is known to code for pain intensity (Büchel et al., 2002; Coghill et al., 2003) and unpleasantness (Rainville et al., 1997), furthermore, sub-divisions (e.g. dorsal anterior ACC) are involved in high level cognitive appraisal of pain, including attention (Büchel et al., 2002). Some have proposed a specific role for dorsal ACC (dACC) in pain perception (Lieberman et al., 2015), though this is disputed with other studies suggesting that activity within this structure reflects the multifaceted nature of pain (Wager et al., 2016). Connectivity

between the ACC and structures involved in descending pain control e.g. the PAG, has been shown to vary with pain perception due to both attentional modulation of pain and placebo analgesic responses (Bantick et al., 2002; Eippert et al., 2009; Petrovic et al., 2000; Valet et al., 2004) suggestive of a role in attentional analgesia. Indeed, cingulotomy has been shown to "disinhibit" noxious heat and cold perception leading to hyperalgesia (Davis et al., 1994).

We hypothesised a top-down pathway mediating attentional analgesia where the PAG receives attentional-shift signals from the ACC and/or LC and directs the RVM and/or LC to attenuate nociceptive processing in the spinal cord. Given the multiplicity of possible pathways and interactions by which activity in the brainstem can generate analgesia, we anticipated that effective connectivity analyses could resolve the roles of these regions (identified in our previous investigation (Brooks et al., 2017)) during attentional analgesia. To increase the statistical power to undertake this connectivity analysis, two further fMRI datasets were acquired using the same paradigm as per Brooks et al. (2017). Analysis of these additional datasets reproduced our previous regional activation results and so the three datasets were pooled for the effective connectivity analyses and modelling. We tested for psycho-physiological interactions (PPI, (Friston et al., 1997; McLaren et al., 2012; O'Reilly et al., 2012) to explore whether the connectivity between the PAG, RVM, LC and ACC altered during the experimental paradigm. Finally, we used dynamic causal modelling (DCM, Friston et al. 2003) to test the directionality and strength of the connections.

Methods

Participants

Subjects were recruited using poster and email adverts at the University of Bristol for three different pain imaging studies at the Clinical Research and Imaging Centre (CRiCBristol) that used the same experimental paradigm: an initial study on attentional analgesia (Brooks et al., 2017), a study on sleep disruption and a study on fibromyalgia. The first two studies were approved by the University Bristol, Faculty of Science, Human Research Ethics Committee (reference 280612567 and 291112606 respectively) and the fibromyalgia study was approved by NHS South Central Oxford B Research Ethics Committee (reference 13/SC/0617).

All subjects gave written informed consent after application of standard inclusion/exclusion criteria for participation in MRI studies. The presence of significant medical/psychiatric disorders (including depression) or pregnancy precluded participation. Subjects with a chronic pain condition, or those who were regularly taking analgesics or psychoactive medications were also excluded. All subjects were right-handed, verified with the Edinburgh handedness inventory (Oldfield, 1971).

The *discovery cohort* were 20 right-handed healthy subjects (median age 25 years, range 18–51 years, 10 females). Subjects attended for two sessions. During the screening visit, written consent was obtained and both task difficulty and temperature of the thermal stimulation were individually calibrated. Subsequently the subjects returned for the test session where they completed the experiment in the MRI scanner (For full details on the *discovery cohort* see Brooks et al., 2017).

The *validation cohort* composed of control subjects from two separate studies:

Twenty healthy volunteers (median age 23, range 20-33, 10 females) were recruited for a study investigating the effects of sleep disturbance on attentional analgesia. Subjects completed the same experiment protocol on two occasions; after a habitual and a disturbed night's sleep (at the sleep

laboratory at CRiCBristol). For the present study, only data obtained from the control condition was used, wherein subjects experienced their habitual sleep regime the night prior to their scan.

A second group of 20 healthy participants (median age 31.5, range 20-59, 18 females) was recruited from the control group of a study analysing attentional analgesia in fibromyalgia patients.

Experiment

Thermal stimuli were delivered to the left volar forearm (approximately C6 dermatome) using a circular contact thermode (CHEPS Pathway, MEDOC) and each lasted 30 seconds. The noxious thermal stimulus was individually titrated to obtain a 6 out of 10 pain rating (42-45˚C plateau). The innocuous stimulus plateau was set at 36˚C. In both cases brief heat spikes of 2, 3 and 4˚C above the plateau temperature were added in a random sequence at a frequency of 1Hz. This heating profile was used to maintain painful perception, whilst avoiding skin sensitisation. The baseline thermode temperature was 32˚C.

For the Rapid Serial Visual Presentation task (RSVP, Potter et al. 1969), subjects identified a visual target (the number "5") among distractors (other letters and numbers), presented using back-projection to a screen, responding with a button box (Lumina LP-400, Cedrus). The speed of character presentation for the hard RSVP task was individually calibrated to obtain a 70% correct detection rate using d', and ranged from 32 to 96 ms. The speed of presentation for the easy RSVP task was either 192 or 256 ms, depending on performance in the hard task (if the "hard" task interval for the subject was <80 ms or >80 ms, respectively).

Data acquisition

In the scanner, participants received noxious or innocuous thermal stimuli (high/low) while simultaneously performing the RSVP task with two levels of difficulty (easy/hard). Thus, there were four experimental conditions (in a 2x2 factorial experimental design): *easy|low*, *easy|high*, *hard|low*, *hard|high*. Each condition was repeated 4 times. Each experimental epoch started with instructions

(5s), followed by the 30s experimental condition, followed by a 10s rest period before an 8s rating period where subjects rated the perceived pain intensity from 0 to 10 on a visual analogue scale (VAS) (See Fig 1 in Brooks et al. 2017). The post-stimulus interval, between the rating period and subsequent instructions, was 17s.

The experiment for the *validation cohort* (n=38) was essentially identical to that of the *discovery cohort*. The titrated mean high temperature for the *discovery cohort* was 44.2˚C and for the *validation cohort* it was 43°C (range 42–45 °C). The whole imaging session lasted 26 minutes for the *discovery cohort* and sleep-disruption cohort and was 22 minutes for the fibromyalgia cohort (as a redundant control condition, with no distraction during high temperature, was omitted).

Imaging was performed with a 3T Skyra MR system (Siemens Medical Solutions, Erlangen, Germany) and 32-channel receive only-head coil. In addition to blood oxygenation level dependent (BOLD) functional data, T1 weighted structural scans were acquired with an MPRAGE sequence to allow image registration. Functional imaging data were acquired with TE/TR=30/3000 ms, GRAPPA acceleration factor = 2, resolution = 1.5 x 1.5 x 3.5 mm. The slices were angulated perpendicularly to the base of the 4th ventricle to improve the acquisition of brainstem nuclei. This slice orientation optimised the ability to discriminate between the small brainstem structures in the transverse plane and while allowing the capture of whole brain activity within 3 seconds. Fieldmap data were acquired with a gradient echo sequence (TE1/TE2/TR = 4.92 / 7.38 / 520 ms, flip angle 60°, resolution 3 x 3 x 3 mm). During scanning, a pulse oximeter and a respiratory bellows (Expression MRI Monitoring System, InVivo, Gainesville, FL) were used to monitor cardiac pulse waveform and respiratory movement for subsequent physiological noise correction (Brooks et al., 2013).

Behavioural Data analysis

Pain VAS ratings were converted to a 0-100 scale for a repeated measures ANOVA in SPSS software (after Brooks et al. 2017). Following estimation of main effects (task, temperature) and interactions, post-hoc paired t-tests were performed. The presence of attentional analgesia was pre-defined as a

significant interaction between task difficulty and high temperature on pain rating on post-hoc paired t-testing ($p < 0.05$). To test for differences between the *discovery* and *validation* cohorts; group membership was added as a between subject factor to the two within subject factors (task and temperature). Subsequent analysis is reported on the *pooled* cohort.

Imaging Data analysis

Image Pre-processing

Functional images were corrected for motion using MCFLIRT (Jenkinson et al., 2012) and co-registered to each subject's structural scan using brain boundary-based registration (Greve et al., 2009) and then to the 2mm template ("MNI152") brain using a combination of fieldmap based unwarping using FUGUE (Jenkinson, 2003), linear transformation using FLIRT (Jenkinson et al., 2001) and non-linear registration using FNIRT (Andersson et al., 2007) with 5mm warp spacing. Functional data were spatially smoothed with a kernel size of 3mm (FWHM) and high pass temporally filtered with a 90s cut-off. Two subjects in the *validation* cohort and one from the *discovery cohort* were excluded from the analyses at this stage because of signal dropout in the EPI data (leaving 57 subjects).

First level analyses

Local autocorrelation correction was performed using FILM (Woolrich et al., 2001) as part of model estimation, which also attempted to correct for physiologically driven signals (originating from cardiac/respiratory processes) using slice-dependent regressors (Brooks et al., 2008; Harvey et al., 2008). The four conditions (*easy*|*high*, *hard*|*high*, *easy*|*low*, *hard*|*low*) and tasks of no interest (cues and rating periods) were modelled using a hemodynamic response function (gamma basis function, $\sigma = 3s$, mean lag = 6s) alongside the physiological regressors within the general linear model in FEAT (Jenkinson et al., 2012). A separate analysis tested for an intra-subject parametric relationship between pain ratings (one per block) and BOLD signal (Büchel et al., 1998). In addition to tasks of

no interest and physiological signal regressors, a constant regressor for all blocks (weighting = 1) and a regressor weighting the individual pain ratings for each block were included. None of the regressors were orthogonalised with respect to any other.

Second level analyses

Main effects were specified as positive and negative main effect of attention (hard versus easy task, and vice versa) and positive and negative main effect of temperature (high versus low thermal stimulus, and vice versa). A task x temperature interaction contrast was also specified. The parametric data was assessed using a simple group average – to examine whether the linear relationship between pain ratings and brain activity was consistent across the group. Lastly, a paired analysis compared activity during the *easy|high* and *hard|high* conditions - to examine whether the inter-subject difference in average pain ratings (i.e. *easy|high* minus *hard|high*) was linearly related to the corresponding difference in BOLD signal (similar to Tracey et al. 2002 and Brooks et al. 2017). To test for differences between the *discovery cohort* and the *validation cohort*, we used an unpaired t test with FLAME (height threshold $z > 3.09$, corrected cluster extent threshold $p < 0.05$), in line with guidelines on corrections for familywise error (FWE) (Eklund et al., 2016). Subsequent analyses of the *pooled* cohort (i.e. all 57 subjects) used the same threshold.

Brainstem-specific analyses

Detecting activation in the brainstem is non-trivial due to its susceptibility to physiological noise and artefacts (Brooks et al., 2013), small size of structures of interest and relative distance from signal detectors in the head coil. Consequently, a brainstem focussed analysis was performed at the group level using a series of anatomical masks and statistical inference using permutation testing in RANDOMISE (Nichols et al., 2002). Analyses utilised pre-defined regions of interest based on (i) a whole brainstem mask derived from the probabilistic Harvard-Oxford subcortical structural atlas (Desikan et al., 2006) and thresholded at 50% and (ii) previously defined probabilistic masks of the *a priori* specified brainstem nuclei (RVM, LC, PAG) from Brooks *et al.* (2017). The number of

permutations were set to 10,000 in line with guidelines (Eklund et al. 2016) and results reported using threshold free cluster enhancement (TFCE) corrected $p < 0.05$ (Smith et al., 2009).

Psycho-Physiological Interactions (PPI)

Effective connectivity analyses were performed on the *pooled cohort*. We used generalised PPI (gPPI) to detect changes in interactions between regions during specific experimental conditions (O'Reilly et al. 2012; McLaren et al. 2012; Friston et al. 1997). In this technique a physiological signal (e.g. the time-course extracted from a seed region) is convolved with a modelled psychological variable (i.e. each one of the experimental conditions) to build an interaction regressor. All interaction regressors were added to a general linear model (GLM) that also included the non-convolved experimental conditions and tasks of no interest (e.g. the rating period). Contrasts were built to test for connectivity differences that could be explained by the main effects of task and temperature and the task * temperature interaction.

Four regions identified in the main effect analyses (temperature and/or attention) in the *pooled cohort*, were selected as seed-regions for the gPPI analysis: PAG, right LC and ACC in the main effect of task and RVM in the main effect of temperature. For each subject, the physiological BOLD time course was extracted from the peak voxel of the pre-processed images (as described in the previous section) within each functional mask, and gPPI performed at the first level. Subsequently, group responses were estimated with permutation testing within the same functional masks e.g. effective connectivity between PAG seed region and the other three regions (RVM, right LC, ACC). For a post hoc investigation of significant results in the task * temperature interaction contrast, we focussed on the conditions of interest (i.e. *easy|high* and *hard|high*). Parameter estimates were extracted by first defining a sphere of radius 2mm at the voxel of greatest significance in the group gPPI result, then back-transforming this mask to subject space and extracting the signal from the voxel with highest Z-score.

In summary, the procedure for gPPI analysis was:

- Time series extraction from functional masks in pre-processed data
- Convolution of time-series with experimental condition
- Building statistical contrasts in a GLM
- First level (single subject) analysis
- Group analysis permutation testing with functional masks
- Extraction of parameter estimates from the conditions of interest.

Dynamic Causal Modelling (DCM)

Given the inability of gPPI to resolve the directionality of connections, we sought to extend our findings by using DCM (Friston et al., 2003). This technique allows the specification of a hypothetical network model (based on equation 1) fitted to the fMRI data to resolve connection strengths.

The change in activity of each region in a model with *j* inputs and *n* brain regions is formalized as follows:

(1)

$$\frac{dx}{dt} = (aA + \sum_{j=1}^{n} u_j bB^j)x + cCu + \omega$$

Where:

x - neuronal state of a region (i.e. BOLD signal convolved with haemodynamic response function)

A - binary vector that defines the connectivity of *x* is to each of the other regions in the model,

a - vector of parameters that define the strengths of such connections,

u - external input to the model,

B - binary vector that defines whether model connections are modulated by external input,

b - vector of parameters that defines the strength of such modulation,

265 *C* - binary vector that defines whether x directly receives the external input,

266 *c* - contains parameters that regulate the strength of the received input,

267 ω - random neuronal noise.

268 Note since the model is estimated in a Bayesian framework, parameters are not single values but are
269 posterior densities.

270 Given the results of the PPI analysis, we specified bi-linear, one state, stochastic, input centred DCMs
271 (Daunizeau et al., 2009; Daunizeau et al., 2012) in SPM 12 (Wellcome Trust Centre for
272 Neuroimaging, London, UK). The models were estimated on a computer cluster (BlueCrystal) in the
273 Advanced Computing Research Centre, University of Bristol – *http://www.bristol.ac.uk/acrc/*.
274 Random effects Bayesian Model Selection (BMS) was used to compare the models and Protected
275 Exceedance Probability, the likelihood of a given model in respect to the others tested, was calculated.
276 Bayesian Omnibus Risk, a measure of the risk of all models having the same frequency within the
277 population, was also computed (Rigoux et al., 2014). Bayesian model averaging (Penny et al., 2010)
278 was used to extract the parameter estimates of interest.

279

Results

Comparison of the discovery cohort and validation cohort

We initially analysed pain scores and main effects of task and temperature on brain activation maps in the *validation cohort* (n=38) independently to qualitatively compare against the results previously obtained in the *discovery cohort* (n=19, Brooks et al., 2017). A two-way repeated measures ANOVA on the pain ratings in the *validation cohort* revealed a main effect of temperature ($F(1, 37) = 137.5$, $P < 0.0001$) and a task x temperature interaction ($F(1, 37) = 24.6$, $P < 0.0001$, Fig. S1), and no main effect of task ($F(1, 37) = 2.1$, $P = 0.15$). A post-hoc paired t-test showed performance of the hard task produced a decrease in pain scores in the high temperature condition (mean *hard*|*high* =39.3, SD 18.9 vs *easy*|*high* =43.6, SD 18.3, $P < 0.001$, Bonferroni corrected), consistent with an attentional analgesic effect (Fig S1).

Analysis of the fMRI activation maps in the *validation cohort* showed a main effect of temperature (*high* versus *low* temperature) in a range of regions including the primary somatosensory cortex, dorsal posterior insula and opercular cortex, with more prominent clusters contralateral to the side of stimulation (applied to the left forearm, Fig S2). In the brainstem, permutation testing with PAG, LC and RVM masks showed activation in all of these nuclei (Fig S2). No cluster reached significance in the negative main effect of temperature (low temperature versus high temperature).

Analysis of the main effect of task (*hard* versus *easy* task) showed bilateral activation in the occipital cortex (Fig S3). The anterior cingulate, anterior insula and paracingulate cortices also showed extensive activation, consistent with the visual attention network (Wager et al., 2004). Activation in the dorsolateral PAG was observed in this whole brain analysis without the need for brainstem-specific masking (Fig S3), presumably because of the increased statistical power afforded by the higher number of subjects compared to Brooks et al. (2017). A permutation test with PAG, LC and RVM masks showed activation in all nuclei (Fig S3). In the reverse contrast (negative main effect of

task, *easy* versus *hard*) main activation clusters were located in the posterior cingulate cortex, frontal medial cortex and in the lateral occipital cortex.

Activation clusters from these main effects analyses are reported in table S1 and, as indicated, were closely consistent with our previous results (Brooks et al, 2017). This qualitative comparison was also assessed quantitatively as follows:

A three-way repeated measures ANOVA on the pain scores using task and temperature as within subject factors and the group (*discovery* vs *validation cohort*) as between subject factor showed no effect of group on the effects of temperature ($P = 0.481$), nor task ($P = 0.833$), nor on the task*temperature interaction ($P = 0.481$).

An unpaired t-test on the functional image contrasts did not show any statistically significant differences between the *discovery* and *validation cohorts* for the main effect of temperature (positive and negative), main effect of task (positive and negative) and interaction contrast (positive and negative).

Given the qualitative similarities and lack of demonstrable statistical differences we went ahead with our planned intention to combine the three datasets and all subsequent results relate to the *pooled cohort* comprising 57 subjects. We also note that the use of strict cluster thresholds for the brain, and of permutation testing for ROI-based analyses in 'noisy' brainstem regions, can produce robust and reproducible results even with a sample size of 20 (Brooks et al, 2017).

Behavioural analysis (Pooled cohort)

The average high (noxious) temperature in the *pooled cohort* was 43.4°C (range 42°C - 45°C). Analysis of the pain ratings showed the expected main effect of temperature ($F(1, 56) = 252.799$, $P < 0.0001$, repeated measures ANOVA) and a task x temperature interaction ($F(1, 56) = 31.969$, $P < 0.0001$, Fig. 1). The main effect of task was not statistically significant ($F(1,56) = 2.935$, $P = 0.092$). A post-hoc paired t-test showed performance of the hard task produced a decrease in pain scores in

the high temperature condition (mean *hard|high* = 38.1, SD 17.0 vs *easy|high* = 42.1, SD 16.5, P < 0.0001, Bonferroni corrected), consistent with an attentional analgesic effect (Fig 1).

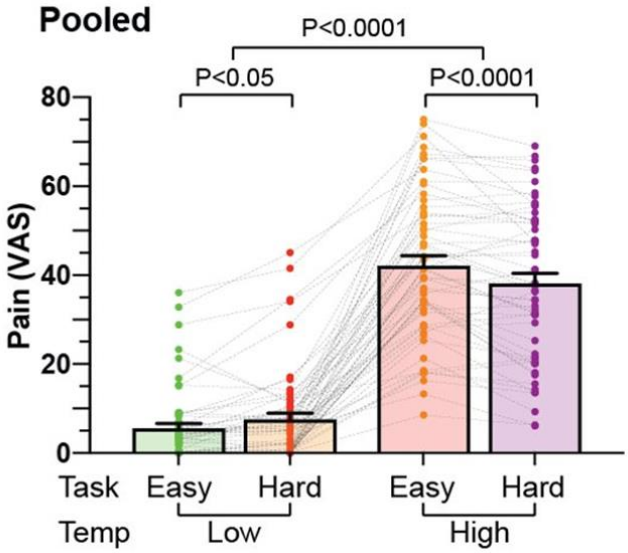

Figure 1. Pain ratings across experimental conditions (means with error bars representing the standard error of the mean) for the pooled cohort. A 2-way repeated measures ANOVA on the pain ratings showed the expected main effect of temperature (P < 0.0001) and a task x temperature interaction (P < 0.0001). A post-hoc paired t-test showed a decrease in pain scores in the high temperature condition during the hard task compared to the easy task (P < 0.0001), showing an analgesic effect caused by the increased cognitive load, as well as an increase in pain scores in the low temperature condition during the hard task compared to the easy task (P < 0.05). The main effect of task was not significant (P = 0.92). Error bars represent the standard error of the mean.

Whole Brain & Brainstem-focussed analysis (Pooled cohort)

Activations were found for the positive main effect of temperature in a range of regions including the anterior and posterior cingulate cortices, precuneus, cerebellum, post-central gyrus (S1), dorsal posterior insula and opercular cortex, in the latter three cases with more prominent clusters contralateral to the side of thermal stimulation (Fig. 2A). In the negative main effect of temperature, significant clusters were found in the frontal medial cortex and in the subcallosal cortex (Fig 2A). At this whole brain level, no clusters of activity were found in the brainstem. To improve our ability to resolve activity in hindbrain structures, we undertook permutation testing using a *whole brainstem*

mask which revealed clusters of activation in the positive main effect of temperature in the ventral PAG, LC bilaterally as well as the RVM (Fig 3A, $p < 0.05$, TFCE corrected).

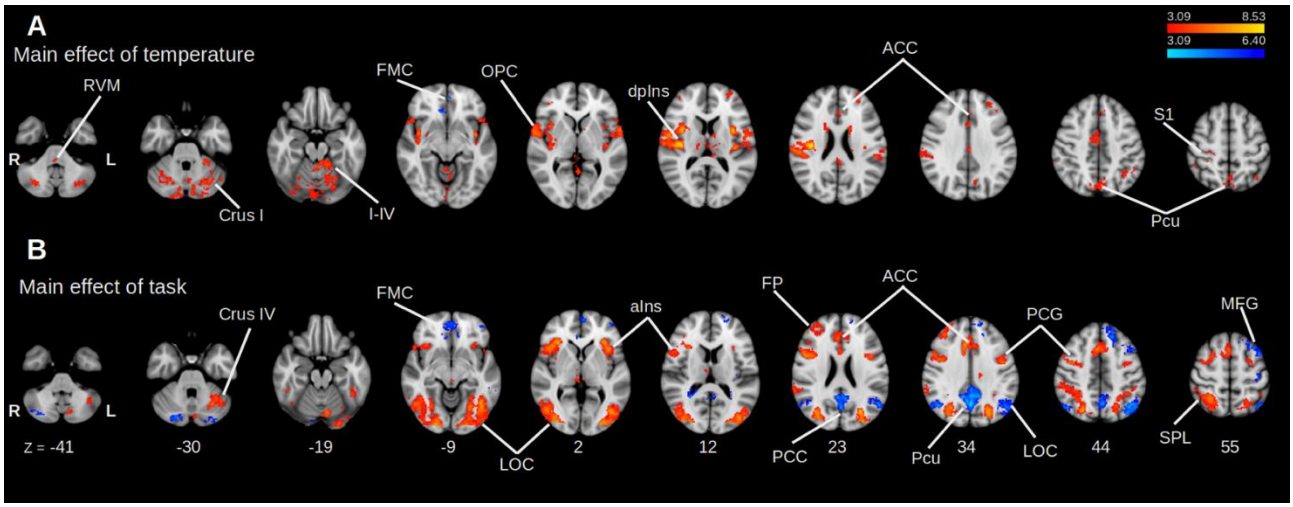

Figure 2. Main effect analyses in the *pooled cohort*, whole brain analysis. Positive (red/yellow) and negative (blue/light-blue). Data was obtained from cluster-based thresholding using an initial threshold of $Z > 3.09$ and FWE corrected $p < 0.05$, one-sample t-test. **(A)** Main effect of temperature. Positive activation in the high temperature conditions was found in anterior cingulate cortex (ACC), thalamus (THAL), dorsal posterior insula (dpIns), precuneus (PCu), primary somatosensory cortex (S1) and rostroventromedial medulla (RVM). Activation in the negative main effect of temperature (low temperature vs high temperature) was observed only in the frontal medial cortex (FMC). **(B)** Main effect of **task**. Activity in the positive main effect was found in the anterior insula (aIns), lateral occipital cortex (LOC), ACC, superior parietal lobule (SPL). Activity in the negative main effect was found in the frontal pole (FP), posterior cingulate cortex (PCC) and Pcu.

Analysis of the positive main effect of task, showed extensive areas of activation within the lateral occipital cortex, superior parietal lobule, anterior cingulate cortex and anterior insula, as well as the PAG (Fig 2B). In the negative main effect of task, clusters were located in the posterior cingulate cortex, frontal medial cortex and in the lateral occipital cortex (Fig 2B). Permutation tests within the *whole brainstem* mask showed multiple clusters of activation, including in the LC bilaterally, RVM and PAG (Fig 3B, $p < 0.05$, TFCE corrected).

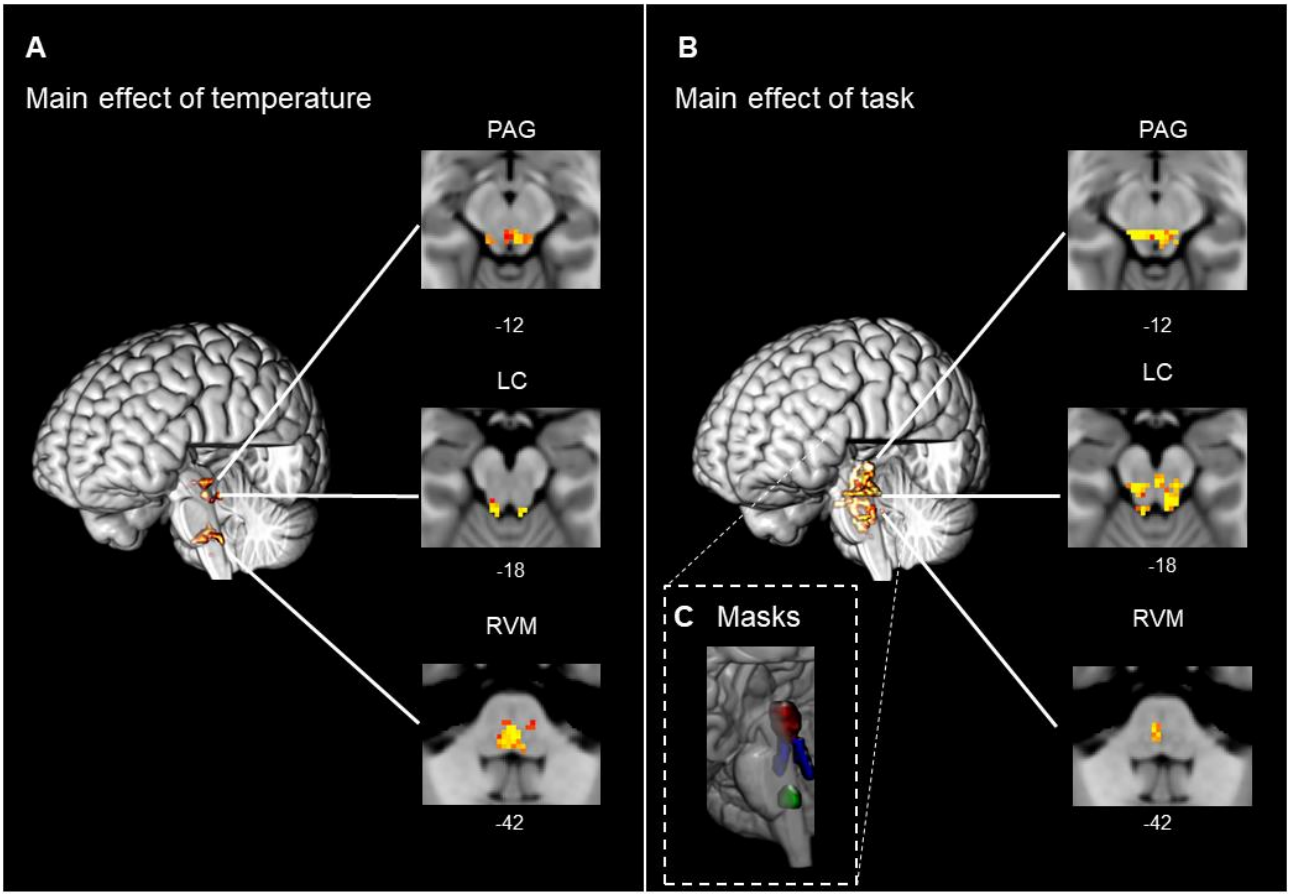

Figure 3. Main effect analyses in the brainstem. Results obtained after permutation testing with a probabilistic *whole brainstem* mask ($p < 0.05$, TFCE corrected). **(A)** Clusters of activation in the brainstem corresponding to the main effect of **temperature** was found in the ventral periaqueductal grey (PAG), rostroventromedial medulla (RVM) and bilateral locus coeruleus (LC). **(B)** Many areas in the superior brainstem show activity in the main effect of **task**, including the PAG, RVM and bilateral LC. **(C)** Anatomical masks defined in (Brooks et al., 2017), identifying the PAG (red), LC (blue), RVM (green).

In the interaction contrast between task and temperature no cluster reached significance either at the whole brain level nor when using the whole brainstem masked analysis.

These findings from the *pooled cohort* showed close similarity to those of Brooks et al. (2017) with the same areas found in the main effects analysis (Table 1 shows all significant clusters). The additional findings at a whole brain level were that both the RVM and the precuneus now appear in the main effect of temperature and the dorsolateral PAG in the main effect of task (the RVM and PAG were only seen in a nucleus specific masked analysis in Brooks et al 2017). Similarly, activity in the brainstem is now seen in more areas using a whole brainstem mask rather than only in the

nucleus specific masks (e.g. main effect of temperature in RVM alone previously versus RVM, LC and PAG in this *pooled* analysis).

Table 1.

Voxels	Z-MAX	X (mm)	Y (mm)	Z (mm)	Atlas labels
Main effect of temperature in the pooled cohort					
2680	8.53	40	-18	18	46% Central Opercular Cortex, 27% Parietal Operculum Cortex, 5% Insular Cortex
2072	5.08	6	-86	-24	3% Occipital Fusiform Gyrus
839	7.03	-36	4	12	61% Central Opercular Cortex, 10% Insular Cortex
386	4.87	0	-70	48	76% Precuneous Cortex
352	4.84	0	20	28	87% Cingulate Gyrus, anterior division
345	6.58	-38	-18	18	50% Central Opercular Cortex, 20% Insular Cortex, 5% Parietal Operculum Cortex
268	5.26	22	-46	72	54% Superior Parietal Lobule, 12% Postcentral Gyrus
265	5.23	32	-26	62	35% Precentral Gyrus, 28% Postcentral Gyrus
238	4.75	4	-26	8	28.2% Right Thalamus
223	4.87	-28	54	18	85% Frontal Pole
133	4.31	4	-26	30	81% Cingulate Gyrus, posterior division
97	4.09	12	-10	18	55.0% Right Thalamus
95	4.7	-34	-56	42	29% Superior Parietal Lobule, 18% Angular Gyrus, 13% Supramarginal Gyrus, posterior division, 12% Lateral Occipital Cortex, superior division
43	4.25	20	16	18	5.8% Right Caudate
42	4.47	36	46	8	47% Frontal Pole

41	4.34	2	-90	-6	34% Lingual Gyrus, 23% Occipital Pole, 13% Intracalcarine Cortex
39	4.73	-26	-50	-50	57.0% Left VIIIa, 35.0% Left VIIIb
36	3.97	-34	32	40	66% Middle Frontal Gyrus, 7% Frontal Pole
34	4.54	-16	8	22	25.6% Left Caudate
34	4.11	-48	-54	46	44% Angular Gyrus, 25% Supramarginal Gyrus, posterior division, 9% Lateral Occipital Cortex, superior division
32	4.8	36	-82	-22	7% Lateral Occipital Cortex, inferior division
32	4.33	48	-44	50	46% Supramarginal Gyrus, posterior division, 17% Angular Gyrus
29	4.31	-4	-40	-44	100.0% Brain-Stem
26	4.3	-48	-64	-30	99.0% Left Crus I
Negative main effect of temperature in the pooled cohort					
67	4.25	6	30	-6	21% Subcallosal Cortex, 13% Cingulate Gyrus, anterior division
28	4.06	-4	46	-12	63% Frontal Medial Cortex, 28% Paracingulate Gyrus
Main effect of task in the pooled cohort					
4948	7.22	22	-90	-8	29.00% Occipital Fusiform Gyrus, 22.00% Occipital Pole, 10.00% Lateral Occipital Cortex, inferior division
4790	7.33	-28	-76	20	41.00% Lateral Occipital Cortex, superior division
3773	7.13	46	16	0	48.00% Frontal Operculum Cortex, 6.00% Insular Cortex
635	6.81	-34	26	0	38.00% Frontal Orbital Cortex, 20.00% Frontal Operculum Cortex, 13.00% Insular Cortex
540	5.26	36	38	36	56.00% Frontal Pole, 23.00% Middle Frontal Gyrus

433	5.87	-42	6	26	27.00% Precentral Gyrus, 26.00% Inferior Frontal Gyrus, pars opercularis
241	6.33	-8	-74	-38	43.0% Left VIIb, 38.0% Left Crus II
205	5.43	4	-26	-2	12.8% Brain-Stem
58	4.68	-46	-38	38	25.00% Supramarginal Gyrus, anterior division, 10.00% Supramarginal Gyrus, posterior division
46	4.65	44	-8	-10	66.00% Planum Polare
45	4.14	-28	-2	58	28.00% Middle Frontal Gyrus, 16.00% Superior Frontal Gyrus, 6.00% Precentral Gyrus
41	5	-38	-52	-44	63.0% Left Crus II, 13.0% Left VIIb, 6.0% Left Crus I
38	5.71	10	-74	-38	57.0% Right Crus II, 18.0% Right VIIb
27	4.52	-14	-22	36	19.00% Cingulate Gyrus, posterior division
Negative main effect of task in the pooled cohort					
1731	6.31	8	-56	30	38% Precuneous Cortex, 20% Cingulate Gyrus, posterior division
1126	6.6	-38	-72	48	68% Lateral Occipital Cortex, superior division
876	5.43	-34	18	56	63% Middle Frontal Gyrus, 2% Superior Frontal Gyrus
511	5.77	32	-70	-36	44.0% Right Crus I, 24.0% Right Crus II
461	5.95	50	-66	40	83% Lateral Occipital Cortex, superior division
346	4.66	6	28	-4	14% Subcallosal Cortex anterior division
257	5.06	-36	-24	70	32% Postcentral Gyrus, 24% Precentral Gyrus
125	4.97	-38	-72	-36	97.0% Left Crus I
94	5.33	-66	-42	-6	54% Middle Temporal Gyrus, posterior division, 29% Middle Temporal Gyrus, temporooccipital part
92	4.99	-16	64	18	82% Frontal Pole

78	4.47	-42	52	2	88% Frontal Pole
41	4.07	-38	-18	18	50% Central Opercular Cortex, 20% Insular Cortex, 5% Parietal Operculum Cortex
38	4.38	-24	-50	18	1% Precuneous Cortex
34	4.16	-64	-8	-14	44% Middle Temporal Gyrus, anterior division, 24% Middle Temporal Gyrus, posterior division, 8% Superior Temporal Gyrus, posterior division

Table 1. Activation clusters from main effects of temperature and distraction in the pooled cohort obtained with cluster-forming threshold Z>3.09 and cluster-corrected p<0.05. The tables were created with Autoaq (part of FSL), with atlas labels based on the degree of overlap with probabilistic atlases (Harvard Oxford Cortical Structural Atlas, Harvard Oxford Subcortical Structural Atlas, Cerebellar Atlas in MNI152 space after normalization with FNIRT). Only those structures to which the cluster had a >5% chance of belonging to are presented.

Linear pain encoding regions

Brain regions whose activity was linearly related to perceived pain intensity were identified using an *intra*-subject parametric regression. This revealed a network of positively correlated regions (similar to those seen in the main effect of temperature) including primarily the right (contralateral) dorsal posterior insula and S1, the anterior cingulate cortex, frontal lobe and the precuneus (Fig 4A). Regions showing a linear decrease in activation with pain ratings were restricted to the occipital cortex bilaterally and ipsilateral primary somatosensory cortex (Fig 4A). Permutation testing in the brainstem (using RVM, PAG and LC masks) identified only the RVM as showing a positive correlation with pain intensity (Fig 4B). No region showed a negative correlation with pain. All these findings were consistent with Brooks *et al* (2017), with the addition of a cluster identified in the thalamus (Table 2).

Regions whose activity correlates with analgesic effect

An *inter*-subject whole-brain mixed effects comparison between the *hard|high* and *easy|high* conditions did not identify any region whose activity linearly correlated with the differences in pain ratings (i.e. analgesia). A parametric regression showed a linear relationship between activity and analgesic effect only in the contralateral (right) LC (i.e. decreased pain ratings were associated with increased BOLD*)*, after permutation testing with LC, RVM and PAG masks (Fig. 4C). A positive relationship was noted between the parameter estimates extracted from the rLC and the attentional analgesic effect on pain scores (Fig 4C).

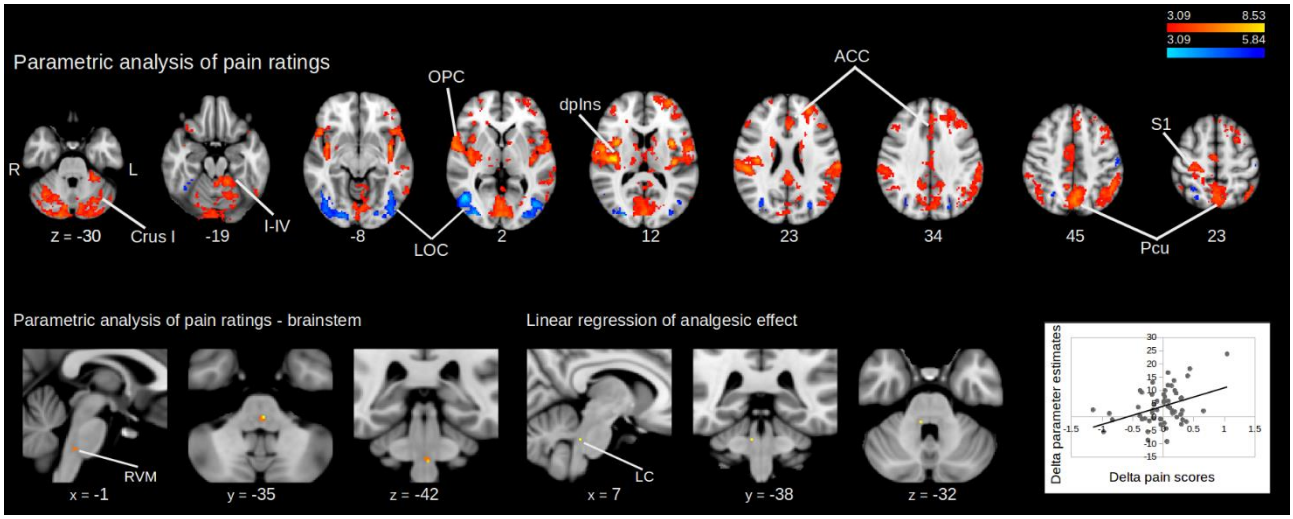

Figure 4. A) Intrasubject parametric regression with pain ratings across all the experimental conditions, in the whole brain. In red-yellow are shown regions whose activity linearly increase with pain ratings, in blue-light blue regions whose activity decreases with the pain ratings. (height threshold $Z > 3.09$, corrected cluster extent threshold $p < 0.05$) **B)** Intrasubject parametric regression with pain ratings, using RVM, LC and PAG masks. Only the RVM shows linear increase in activity with the pain scores ($p < 0.05$, TFCE corrected). **C)** Inter-subject parametric regression with the analgesic effect (i.e. ratings of *easy|high* – *hard|high*), using a LC mask ($p < 0.05$, TFCE corrected).

419 **Table 2.**

Voxels	Z-MAX	X (mm)	Y (mm)	Z (mm)	Atlas labels
Positive relationship with pain ratings					
9467	6.36	32	-28	64	40% Postcentral Gyrus, 26% Precentral Gyrus
3621	8.37	40	-18	18	46% Central Opercular Cortex, 27% Parietal Operculum Cortex, 5% Insular Cortex
3481	7.78	-56	-2	8	45% Central Opercular Cortex, 28% Precentral Gyrus, 5% Planum Polare
1693	5.93	-26	46	26	79% Frontal Pole
287	4.98	-62	-56	-10	54% Middle Temporal Gyrus, temporooccipital part, 21% Inferior Temporal Gyrus, temporooccipital part, 7% Lateral Occipital Cortex, inferior division
285	5.2	4	-26	8	28.2% Right Thalamus
120	4.42	20	-8	28	3.1% Right Caudate
95	4.18	42	48	8	80% Frontal Pole
86	4.71	16	-20	10	099.8% Right Thalamus
71	5.79	-26	-50	-50	57% Left VIIIa, 35% Left VIIIb
59	4.41	46	26	36	65% Middle Frontal Gyrus
46	3.82	-20	-28	68	39% Precentral Gyrus, 23% Postcentral Gyrus
38	4.17	-42	-72	24	72% Lateral Occipital Cortex, superior division
37	4.11	-18	-38	66	51% Postcentral Gyrus
36	3.84	2	-66	-38	69% Vermis VIIIa, 13% Vermis VIIIb
34	3.83	24	54	26	76% Frontal Pole
33	4.48	52	30	22	32% Middle Frontal Gyrus, 30% Inferior Frontal Gyrus, pars triangularis

31	3.78	28	58	0	76% Frontal Pole
Negative relationship with pain ratings					
1637	6.16	46	-64	2	56% Lateral Occipital Cortex, inferior division, 10% Middle Temporal Gyrus, temporooccipital part
1184	5.36	-42	-74	0	63% Lateral Occipital Cortex, inferior division
176	5.38	-26	-76	30	67% Lateral Occipital Cortex, superior division
126	4.73	26	-52	50	34% Superior Parietal Lobule, 3% Lateral Occipital Cortex, superior division
51	4.32	-54	-16	52	57% Postcentral Gyrus, 8% Precentral Gyrus

Table 2. Results from intrasubject parametric regression with pain ratings in the *pooled cohort* obtained with cluster-forming threshold Z>3.09 and cluster-corrected p<0.05. The tables were created with Autoaq (part of FSL), with atlas labels based on the degree of overlap with probabilistic atlases (Harvard Oxford Cortical Structural Atlas, Harvard Oxford Subcortical Structural Atlas, Cerebellar Atlas in MNI152 space after normalization with FNIRT). Only those structures to which the cluster had a >5% chance of belonging to are presented.

gPPI analysis

The analysis aimed to identify changes in effective connectivity associated with altered task difficulty, temperature and the task x temperature interaction. The previous main effect analyses provided us with functional activation masks that were used to extract time courses for these gPPI analyses; in the RVM for the main effect of temperature, and in the PAG, rLC and ACC for the main effect of task (see Methods). Permutation testing revealed increased connectivity with the following contrasts (Fig 5):

- RVM seed - increased connectivity to PAG for the interaction contras
- ACC seed - increased connectivity with the right (contralateral) LC in the interaction contrast and with the PAG in the main effect of task

- PAG seed - did not show any significant change in effective connectivity
- rLC seed - did not show any significant change in effective connectivity.

For all gPPI results, parameter estimates were extracted from the voxel with greatest significance in each individual to explore the nature of these interactions (Fig 5B). In all cases, the parameter estimates were greater in the *hard|high* compared to the *easy|high* condition, indicating an increase in coupling in the circumstances producing analgesia.

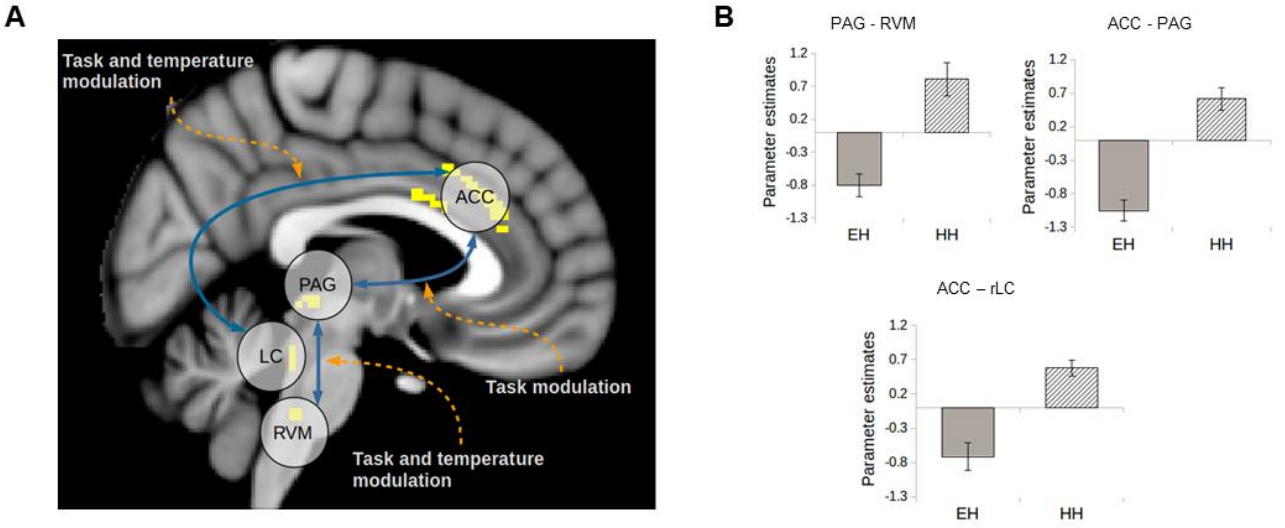

Figure 5 (A) Schematic representation of results of the PPI analysis. Results were obtained with single-nucleus functional masks and permutation testing ($P < 0.05$, TFCE corrected). **(B)** Parameter estimates extracted from the peak destination voxel from the PPI analysis (see text for details), in the *easy|high* and *hard|high* conditions.

DCM

The connections resolved in the gPPI were further examined with DCM to resolve the directionality of the task effect. We systematically varied the location of the task inputs and modulation, while the temperature modulation was kept fixed in all models as a bottom-up effect. External inputs were both hard/easy task and high/low temperature, while modulations were only hard task and high temperature. Five models were specified (Fig 6A):

1) No modulation of connections,
2) Task was bottom-up on the ACC-PAG-RVM and on the ACC-LC axis.
3) Task was top-down for both pathways.
4) Task was top-down in the ACC-PAG-RVM axis and bottom-up in the ACC-LC connection.
5) Task was bottom-up in ACC-PAG-RVM and top-down in ACC-LC.

Models 3 and 4 were found to best fit the data in BMS, with protected exceedance probability = 0.45 and 0.55 respectively (Fig 6B), and Bayesian omnibus risk of zero. In both, the task had a top-down influence on ACC-PAG-RVM, while the ACC-LC connection was top-down modulated in one model and bottom-up modulated in the other. Bayesian model averaging was used to extract parameter estimates (Table 3).

All connections were also tested with an analgesic covariate, to find whether one or more consistently differed in participants that showed an analgesic effect. No connection reached significance in this test.

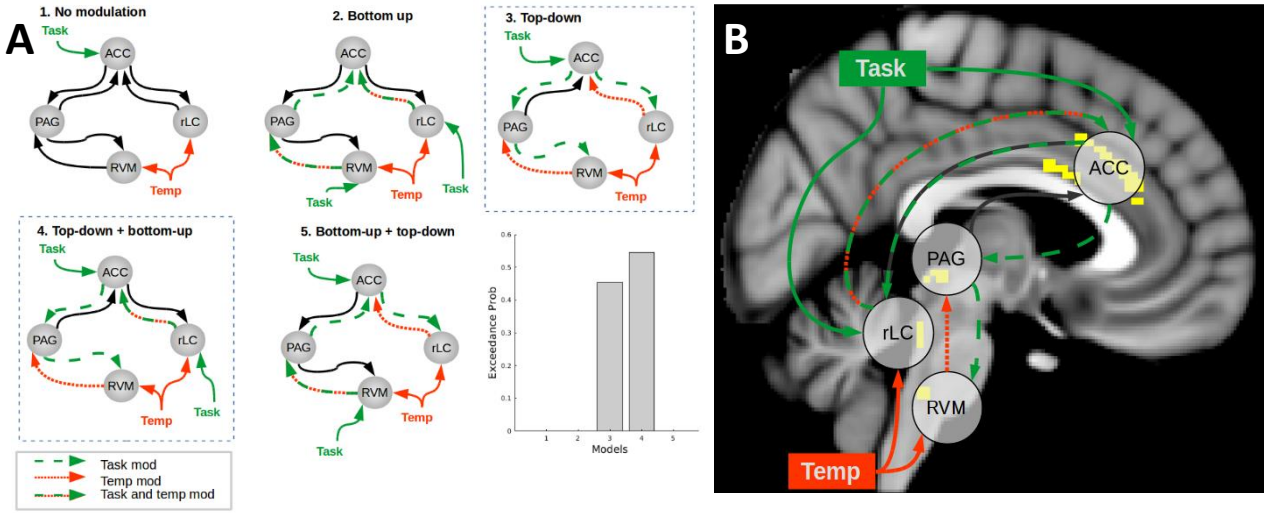

Figure 6 (A) Specified models and result of Bayesian Model Selection. The effect of temperature is always bottom-up, while the task could have a bottom-up or top-down effect. Model 3 and 4 have the strongest evidence of reproducing the data, with slightly stronger evidence for model 4. (B) Schematic representation of interactions during attentional analgesia, after PPI and DCM.

Table 3.

Parameter	Parameter estimate mean (SD)	Task modulation mean (SD)
ACC-PAG connection	0.084 (0.0012)	0.029 (0.0052)
ACC-LC connection	0.058 (0.0011)	-0.019 (0.0054)
PAG-ACC connection	0.083 (0.0012)	-0.0058 (0.0026)
PAG-RVM connection	0.039 (0.0011)	-0.038 (0.0061)
LC-ACC connection	0.054 (0.0012)	-0.012 (0.0052)
RVM-PAG connection	0.034 (0.0012)	-0.0004 (0.0026)

Table 3. Summary of mean parameter estimates for connections and task modulation in DCM.

Discussion

In the context of a reproducibility crisis that is afflicting neuroscience, especially in fMRI experiments (Button et al., 2013; Eklund et al., 2016), we report results that have reproduced and extended the generalisability of the key findings regarding the neural substrates of attentional analgesia that were originally reported in Brooks et al., 2017. The same subset of brain regions was shown to be involved in the performance of a visual attention task and in pain perception. Importantly, we replicated the involvement in attentional analgesia of brainstem structures such as PAG, LC and RVM. This was demonstrable without the need for region specific anatomical masks because we increased our resolving power by analysing a larger cohort of subjects. By using gPPI and DCM analyses we demonstrated changes in effective connectivity between these key brainstem regions and the ACC, that are likely involved in the mediation of attentional analgesia.

The higher statistical power provided by 57 subjects, some 3-fold greater than in Brooks et al. (2017), yielded stronger findings especially in the brainstem nuclei. For the main effect of temperature, we were now able to see activation in the RVM at a whole brain analysis level. Additionally, using a full brainstem mask (rather than region specific masks) we found activation not only in the RVM, as previously (Brooks et al., 2017), but also in PAG and bilaterally in LC. While it has long been known from animal studies that these brainstem regions receive nociceptive input from the spinal cord (Blomqvist & Craig, 1991; Cedarbaum & Aghajanian, 1978; Keay et al., 1997) this has seldom been clearly demonstrated in human imaging studies. The specificity of this pattern of nociceptive information flow is striking with activations confined to discrete territories including ventral PAG, LC and RVM as well as activations in the region of parabrachial nucleus, nucleus solitarius, sub nucleus reticularis dorsalis and nucleus cuneiformis. The intra-subject linear regression analysis with pain scores in regions such as the dorsal posterior insula and the anterior cingulate cortex, where the BOLD signal linearly scales with perceived pain, was also consistent with previous results (Horing et al., 2019). In the brainstem, the only region showing the same linear relationship is the RVM. This clearly demonstrates that this brainstem territory is likely to be playing an important role in coding

nociceptive intensity. To our knowledge, no other single study has been able to produce such a complete activation map in the human brainstem in response to noxious stimulation (see review by Henderson & Keay, 2018).

Considering the main effect of task, we were now able to identify activity in the PAG at the whole brain level. By using a whole brainstem mask, we were able to detect activity in RVM and LC bilaterally (as well as the dorsal PAG), while in our previous study using region specific masks we could only find responses in the right LC and PAG (Brooks et al., 2017). It is interesting to note that the attention task recruited the dorsal and ventral PAG whereas the noxious input produced activation in the ventral region of the nucleus perhaps in line with the known behavioural specialisation of columns within this crucial integrating nucleus (Linnman et al., 2012; Roy et al., 2014).

The magnitude of the analgesic effect showed a correlation with activity in the right LC (a finding that we previously noted in Brooks et al. (2017) but was just below formal statistical significance). This was the only location in the neuroaxis that showed this relationship. The LC is well positioned both anatomically and functionally to mediate a component of attentional analgesia, not only because it is responsive to attentional states and cognitive task performance (Aston-Jones & Cohen, 2005; Sales et al., 2019; Sara, 2009; Yu & Dayan, 2005) and to nociceptive inputs (Cedarbaum & Aghajanian, 1978; Howorth et al., 2009), but also particularly in being able to cause analgesia via its direct spinal cord projections (Hirschberg et al., 2017; Jones et al., 1986). Intriguingly, the spinal cord-projecting neurons are located in the caudal part of the LC in rodents (Hirschberg et al., 2017), as is the LC region that we found to correlate with the analgesic effect. Previous analyses have demonstrated linear relationships between the analgesic effect and activity located in the PAG in 9 subjects (Tracey et al., 2002) and RVM in 20 subjects (Brooks et al., 2017). We note that neither of these findings were replicated our current study of 57 subjects. While all three findings are biologically plausible, a large sample size seems necessary to produce robust results with inter-subject regression (especially in small, noisy brainstem nuclei) and this is likely to be complicated by the known interactions between these regions in nociceptive processing (discussed below).

To examine interplay between the cortical and brainstem structures we hypothesised to be involved in attentional analgesia, we performed a generalised PPI, which determines how connectivity changes as a result of experimental manipulation (i.e. effective connectivity). Our prior hypothesis for a role of the ACC was supported by the observation that it showed overlapping areas of activation in both conditions. We observed altered connectivity between the ACC and contralateral (right) LC during the interaction between task and temperature. Parameter estimates extracted from voxels showing this interaction revealed that coupling was enhanced during the hard task/high temperature condition. Furthermore, coupling increased between ACC and PAG with task demand, and between PAG and RVM, during the task x temperature interaction. Extraction of parameter estimates revealed that, as for ACC-LC connection, this PAG-RVM interaction was enhanced in the hard task/high temperature condition.

Effective connectivity changes in these pathways may therefore mediate the process of attentional analgesia. This could be achieved through LC projections to the ACC increasing the signal-to-noise (or salience) of one input over another (Manella et al., 2017; Muller et al., 2019; Sales et al., 2019; Sara, 1985; Vazey et al., 2018) and/or ACC to spinally projecting LC neurons modulating the activity of dorsal horn neurons (i.e. decreasing nociceptive transmission) both actions potentially giving 'precedence' to the task. One intriguing aspect of this interaction is the lateralised nature of relationship between the right LC and the analgesic effect (i.e. contralateral to the stimulus) - a finding that has previously been noted in rodent studies where noxious stimuli increase the activity in the contralateral LC to a greater effect (Cedarbaum et al., 1978). Similarly, the reduction in perceived pain could equally be via ACC recruiting the PAG and RVM to produce antinociception at a spinal level during the demanding attentional task (Millan, 2002). This conceptually extends previous studies that have identified the ACC-PAG connection as being involved in a distraction from pain (attentional analgesia) paradigm (Valet et al., 2004), as well as in a placebo analgesia paradigm (Petrovic, 2002). The PAG-RVM descending control system has also already been implicated in placebo analgesia (Eippert et al., 2009; Grahl et al., 2018) via an opioid-dependent mechanism. The

554 behavioural component of attentional analgesia has been reported to be impaired by opioid blockade,
555 possibly by disrupting connections between the ACC-PAG-RVM descending control system
556 (Sprenger et al., 2012).

557 We used dynamic causal modelling to resolve the directionality of the connection changes that were
558 shown in the gPPI, with the objective of better characterising the network mechanism generating
559 analgesia. We employed stochastic DCM, which allows for modelling of random neuronal noise in
560 the system, to improve network resolution in brainstem areas significantly affected by physiological
561 noise (Brooks et al., 2013). This routine was shown to improve the characterization of network
562 structure and parameter inference over deterministic DCM (Daunizeau et al., 2012; Osório et al.,
563 2015) and has been widely used in resting state and task-based fMRI studies since its release (Kahan
564 et al., 2014; Ma et al., 2015, 2014; Ray et al., 2016; Zhang et al., 2015). Bayesian Model selection
565 validated the results of the gPPI by excluding, for lack of evidence, a model where no connection was
566 modulated by task. We resolved a top-down influence of task on the ACC-PAG and PAG-RVM
567 connections, consistent with a descending pain modulatory system being involved in attentional
568 analgesia (Sprenger et al., 2012). The ACC-LC pathway was however not resolved as clearly, with
569 similar evidence in BMS for task modulation of the top-down and bottom-up connection. As
570 discussed above, both possibilities are supported by solid biological evidence and it is possible that
571 the two regions work in a feedback loop during attentional analgesia. On examination of the
572 parameter estimates, it was noted that the task modulation had a negative effect on all connections,
573 except for ACC-PAG. This is consistent with a reciprocal negative feedback loop between ACC and
574 LC (Breton-Provencher et al., 2019; Ramos et al., 2007), and with a disinhibition of the RVM "off-
575 cells" by the PAG (Lau et al., 2014). It is quite conceivable that the parallel ACC-LC and ACC-
576 PAG-RVM systems described here work in concert to cause analgesia. Previous animal studies show
577 that electrical stimulation of the PAG triggers noradrenaline release in the cerebrospinal fluid (Cui et
578 al., 1999; Hammond et al., 1985) and the analgesic effect of stimulation can be partially blocked with
579 intrathecal alpha2 antagonists.

We propose that the ACC acts to resolve the conflict caused by an attention-grabbing painful stimulus and the cognitive demands of a sustained visual attention task, by sending downstream signals to brainstem structures to facilitate optimal behaviour. Intriguingly, inputting the coordinates of the peak attentional activation of the ACC to Neurosynth (Yarkoni et al., 2011) identified three studies where the same region was involved in response to conflict (Barch et al., 2001; Scholl et al., 2017; van Veen et al., 2005; Wittfoth et al., 2008). In addition, voluntary control over the activation of this area was shown to result in modulation of pain perception in a neurofeedback study (deCharms et al., 2005). This network is also relevant for mindfulness-based techniques, where focus on an internal signal (e.g. breathing), effectively distracts subjects from the painful stimulus. Interestingly, mindfulness mediated pain relief is not mediated by endogenous opioids (Zeidan et al., 2016) but relies on the rACC (Zeidan et al., 2012; Zeidan & Vago, 2016), perhaps through the ACC-LC pathway.

In this study we have been able to resolve parallel cortical – brainstem pathways that form a network that is functionally engaged when pain perception is attenuated during attentional analgesia. We note that the spinal cord BOLD response to nociception has previously been shown to be modulated by attention (Sprenger et al., 2012). Whether this spinal modulation of nociception is the product of activation of the ACC-PAG-RVM and/or the ACC-LC system still needs to be demonstrated in humans. It is known that both pathways could involve opioids (Fields, 2004) and so previous studies using naloxone do not discriminate between these possibilities. A connectivity analysis examining the network activity between cortical territories, brainstem nuclei and dorsal horn *in toto* may help to define the key pathway in attentional analgesia. We further postulate that this network may be of importance in chronic conditions where disruption of attention and cognition (i.e. fibromyalgia) are co-morbid alongside pain.

602 **Bibliography**

Andersson, J. L. R., Jenkinson, M., & Smith, S. (2007). Non-linear registration aka Spatial normalisation. *FMRIB Technial Report TR07JA2*.

Astafiev, S. V, Snyder, A. Z., Shulman, G. L., & Corbetta, M. (2010). Comment on "Modafinil shifts human locus coeruleus to low-tonic, high-phasic activity during functional MRI" and "Homeostatic sleep pressure and responses to sustained attention in the suprachiasmatic area". *Science (New York, N.Y.)*, *328*(5976), 309; author reply 309. https://doi.org/10.1126/science.1177200

Aston-Jones, G., & Cohen, J. D. (2005). An Integrative Theory of Locus Coeruleus-Norepinephrine Function: Adaptive Gain and Optimal Performance. *Annual Review of Neuroscience*, *28*(1), 403–450. https://doi.org/10.1146/annurev.neuro.28.061604.135709

Aston-Jones, G., Rajkowski, J., & Cohen, J. (1999). Role of locus coeruleus in attention and behavioral flexibility. *Biological Psychiatry*, *46*(9), 1309–1320. Retrieved from http://www.ncbi.nlm.nih.gov/pubmed/10560036

Aston-Jones, G., Shipley, M. T., Chouvet, G., Ennis, M., van Bockstaele, E., Pieribone, V., … Williams, J. T. (1991). Afferent regulation of locus coeruleus neurons: anatomy, physiology and pharmacology. *Progress in Brain Research*, *88*, 47–75. https://doi.org/10.1016/S0079-6123(08)63799-1

Bajic, D., & Proudfit, H. K. (1999). Projections of neurons in the periaqueductal gray to pontine and medullary catecholamine cell groups involved in the modulation of nociception. *The Journal of Comparative Neurology*, *405*(3), 359–379. Retrieved from http://www.ncbi.nlm.nih.gov/pubmed/10076931

Bantick, S. J., Wise, R. G., Ploghaus, A., Clare, S., Smith, S. M., & Tracey, I. (2002). Imaging how attention modulates pain in humans using functional MRI. *Brain*, *125*(2), 310–319. https://doi.org/10.1093/brain/awf022

Barch, D. M., Braver, T. S., Akbudak, E., Conturo, T., Ollinger, J., & Snyder, A. (2001). Anterior

cingulate cortex and response conflict: effects of response modality and processing domain. *Cerebral Cortex (New York, N.Y. : 1991)*, *11*(9), 837–848. Retrieved from http://www.ncbi.nlm.nih.gov/pubmed/11532889

Basbaum, A. I., & Fields, H. L. (1979). The origin of descending pathways in the dorsolateral funiculus of the spinal cord of the cat and rat: Further studies on the anatomy of pain modulation. *Journal of Comparative Neurology*, *187*(3), 513–531. https://doi.org/10.1002/cne.901870304

Blomqvist, A., & Craig, A. D. (1991). Organization of Spinal and Trigeminal Input to the PAG. In *The Midbrain Periaqueductal Gray Matter* (pp. 345–363). https://doi.org/10.1007/978-1-4615-3302-3_19

Braver, T. S., Barch, D. M., Gray, J. R., Molfese, D. L., & Snyder, A. (2001). Anterior Cingulate Cortex and Response Conflict: Effects of Frequency, Inhibition and Errors. *Cerebral Cortex*, *11*(9), 825–836. https://doi.org/10.1093/cercor/11.9.825

Breton-Provencher, V., & Sur, M. (2019). Active control of arousal by a locus coeruleus GABAergic circuit. *Nature Neuroscience*, *22*(2), 218–228. https://doi.org/10.1038/s41593-018-0305-z

Brooks, Davies, & Pickering. (2017). Resolving the brainstem contributions to attentional analgesia in man. *The Journal of Neuroscience*. https://doi.org/10.1523/JNEUROSCI.2193-16.2016

Brooks, J. C. W., Beckmann, C. F., Miller, K. L., Wise, R. G., Porro, C. A., Tracey, I., & Jenkinson, M. (2008). Physiological noise modelling for spinal functional magnetic resonance imaging studies. *NeuroImage*, *39*(2), 680–692. https://doi.org/10.1016/j.neuroimage.2007.09.018

Brooks, J. C. W. P., Faull, O. K., Pattinson, K. T. S. Dp. F., Jenkinson, M. P., & Beissner, F. (2013). Physiological noise in brainstem fMRI. *Frontiers in Human Neuroscience*, *7*(October), 623. https://doi.org/10.3389/fnhum.2013.00623

Brooks, J. W. C. W., Nurmikko, T. J., Bimson, W. E., Singh, K. D., & Roberts, N. (2002). fMRI of

thermal pain: Effects of stimulus laterality and attention. *NeuroImage*, *15*(2), 293–301. https://doi.org/10.1006/nimg.2001.0974

Büchel, C., Bornhövd, K., Quante, M., Glauche, V., Bromm, B., & Weiller, C. (2002). Dissociable Neural Responses Related to Pain Intensity, Stimulus Intensity, and Stimulus Awareness within the Anterior Cingulate Cortex: A Parametric Single-Trial Laser Functional Magnetic Resonance Imaging Study. *The Journal of Neuroscience*, *22*(3), 970–976. https://doi.org/10.1523/JNEUROSCI.22-03-00970.2002

Büchel, C., Holmes, A. P., Rees, G., & Friston, K. J. (1998). Characterizing stimulus-response functions using nonlinear regressors in parametric fMRI experiments. *NeuroImage*, *8*(2), 140–148. https://doi.org/10.1006/nimg.1998.0351

Bushnell, M. C., Čeko, M., & Low, L. A. (2013). *Cognitive and emotional control of pain and its disruption in chronic pain*. https://doi.org/10.1038/nrn3516

Button, K. S., Ioannidis, J. P. A., Mokrysz, C., Nosek, B. A., Flint, J., Robinson, E. S. J., & Munafò, M. R. (2013). Power failure: why small sample size undermines the reliability of neuroscience. *Nature Reviews Neuroscience*, *14*(5), 365–376. https://doi.org/10.1038/nrn3475

Cedarbaum, J. M., & Aghajanian, G. K. (1978). Activation of locus coeruleus neurons by peripheral stimuli: Modulation by a collateral inhibitory mechanism. *Life Sciences*, *23*(13), 1383–1392. https://doi.org/10.1016/0024-3205(78)90398-3

Coghill, R. C., McHaffie, J. G., & Yen, Y. F. (2003, July 8). Neural correlates of interindividual differences in the subjective experience of pain. *Proceedings of the National Academy of Sciences of the United States of America*, Vol. 100, pp. 8538–8542. https://doi.org/10.1073/pnas.1430684100

Crombez, G., Eccleston, C., Van den Broeck, A., Goubert, L., & Van Houdenhove, B. (2004). Hypervigilance to pain in fibromyalgia: the mediating role of pain intensity and catastrophic thinking about pain. *The Clinical Journal of Pain*, *20*(2), 98–102. Retrieved from http://www.ncbi.nlm.nih.gov/pubmed/14770049

Cui, M., Feng, Y., McAdoo, D. J., & Willis, W. D. (1999). Periaqueductal gray stimulation-induced inhibition of nociceptive dorsal horn neurons in rats is associated with the release of norepinephrine, serotonin, and amino acids. *The Journal of Pharmacology and Experimental Therapeutics*, *289*(2), 868–876. Retrieved from http://www.ncbi.nlm.nih.gov/pubmed/10215665

Daunizeau, J., Stephan, K. E., & Friston, K. J. (2012). Stochastic dynamic causal modelling of fMRI data: should we care about neural noise? *NeuroImage*, *62*(1), 464–481. https://doi.org/10.1016/j.neuroimage.2012.04.061

Davis, K. D., Hutchison, W. D., Lozano, A. M., & Dostrovsky, J. O. (1994). Altered pain and temperature perception following cingulotomy and capsulotomy in a patient with schizoaffective disorder. *Pain*, *59*(2), 189–199. https://doi.org/10.1016/0304-3959(94)90071-X

Davis, K. D., Hutchison, W. D., Lozano, A. M., Tasker, R. R., & Dostrovsky, J. O. (2000). Human Anterior Cingulate Cortex Neurons Modulated by Attention-Demanding Tasks. *Journal of Neurophysiology*, *83*(6), 3575–3577. https://doi.org/10.1152/jn.2000.83.6.3575

De Felice, M., & Ossipov, M. H. (2016). Cortical and subcortical modulation of pain. *Pain Management*, *6*(2), 111–120. https://doi.org/10.2217/pmt.15.63

deCharms, R. C., Maeda, F., Glover, G. H., Ludlow, D., Pauly, J. M., Soneji, D., … Mackey, S. C. (2005). Control over brain activation and pain learned by using real-time functional MRI. *Proceedings of the National Academy of Sciences of the United States of America*, *102*(51), 18626–18631. https://doi.org/10.1073/pnas.0505210102

Desikan, R. S., Ségonne, F., Fischl, B., Quinn, B. T., Dickerson, B. C., Blacker, D., … Killiany, R. J. (2006). An automated labeling system for subdividing the human cerebral cortex on MRI scans into gyral based regions of interest. *NeuroImage*, *31*(3), 968–980. https://doi.org/10.1016/J.NEUROIMAGE.2006.01.021

Eccleston, C., & Crombez, G. (1999). Pain demands attention: A cognitive–affective model of the interruptive function of pain. *Psychological Bulletin*, *125*(3), 356–366.

https://doi.org/10.1037/0033-2909.125.3.356

Eippert, F., Bingel, U., Schoell, E. D., Yacubian, J., Klinger, R., Lorenz, J., & Büchel, C. (2009). Activation of the Opioidergic Descending Pain Control System Underlies Placebo Analgesia. *Neuron*, *63*(4), 533–543. https://doi.org/10.1016/j.neuron.2009.07.014

Eklund, A., Nichols, T. E., & Knutsson, H. (2016). Cluster failure: Why fMRI inferences for spatial extent have inflated false-positive rates. *Proceedings of the National Academy of Sciences of the United States of America*, *113*(28), 7900–7905. https://doi.org/10.1073/pnas.1602413113

Eklund, A., Nichols, T. E., & Knutsson, H. (2016). Cluster failure: Why fMRI inferences for spatial extent have inflated false-positive rates. *Proceedings of the National Academy of Sciences of the United States of America*, *113*(28), 7900–7905. https://doi.org/10.1073/pnas.1602413113

Fields, H. (2004). State-dependent opioid control of pain. *Nature Reviews Neuroscience*. https://doi.org/10.1038/nrn1431

Fields, H. L., & Basbaum, A. I. (1978). Brainstem control of spinal pain-transmission neurons. *Annual Review of Physiology*.

Friston, K. . J., Buechel, C., Fink, G. . R., Morris, J., Rolls, E., & Dolan, R. . J. (1997). Psychophysiological and modulatory interactions in neuroimaging. *NeuroImage*, *6*(3), 218–229. https://doi.org/10.1006/nimg.1997.0291

Friston, K. J., Buechel, C., Fink, G. R., Morris, J., Rolls, E., & Dolan, R. J. (1997). Psychophysiological and modulatory interactions in neuroimaging. *NeuroImage*, *6*(3), 218–229. https://doi.org/10.1006/nimg.1997.0291

Friston, K. J., Harrison, L., & Penny, W. (2003). Dynamic causal modelling. *NeuroImage*, *19*(4), 1273–1302. https://doi.org/10.1016/S1053-8119(03)00202-7

Garcia-Larrea, L., & Peyron, R. (2013). Pain matrices and neuropathic pain matrices: A review. *Pain*, *154*, S29–S43. https://doi.org/10.1016/j.pain.2013.09.001

Grahl, A., Onat, S., & Büchel, C. (2018). The periaqueductal gray and Bayesian integration in placebo analgesia. *ELife*, *7*. https://doi.org/10.7554/eLife.32930

Greve, D. N., & Fischl, B. (2009). Accurate and robust brain image alignment using boundary-based registration. *NeuroImage*, *48*(1), 63–72. https://doi.org/10.1016/j.neuroimage.2009.06.060

Hammond, D. L., Tyce, G. M., & Yaksh, T. L. (1985). Efflux of 5-hydroxytryptamine and noradrenaline into spinal cord superfusates during stimulation of the rat medulla. *The Journal of Physiology*, *359*, 151–162. Retrieved from http://www.ncbi.nlm.nih.gov/pubmed/2582112

Harvey, A. K., Pattinson, K. T. S., Brooks, J. C. W., Mayhew, S. D., Jenkinson, M., & Wise, R. G. (2008). Brainstem functional magnetic resonance imaging: disentangling signal from physiological noise. *Journal of Magnetic Resonance Imaging : JMRI*, *28*(6), 1337–1344. https://doi.org/10.1002/jmri.21623

Heinricher, M. M., Tavares, I., Leith, J. L., & Lumb, B. M. (2009). Descending control of nociception: Specificity, recruitment and plasticity. *Brain Research Reviews*, *60*(1), 214–225. https://doi.org/10.1016/j.brainresrev.2008.12.009

Henderson, L. A., & Keay, K. A. (2018). Imaging Acute and Chronic Pain in the Human Brainstem and Spinal Cord. *The Neuroscientist*, *24*(1), 84–96. https://doi.org/10.1177/1073858417703911

Hirschberg, S., Li, Y., Randall, A., Kremer, E. J., & Pickering, A. E. (2017). Functional dichotomy in spinal- vs prefrontal-projecting locus coeruleus modules splits descending noradrenergic analgesia from ascending aversion and anxiety in rats. *ELife*, *6*, e29808. https://doi.org/10.7554/eLife.29808

Horing, B., Sprenger, C., & Büchel, C. (2019). The parietal operculum preferentially encodes heat pain and not salience. *PLOS Biology*, *17*(8), e3000205. https://doi.org/10.1371/journal.pbio.3000205

Howorth, P. W., Teschemacher, A. G., & Pickering, A. E. (2009). Retrograde adenoviral vector targeting of nociresponsive pontospinal noradrenergic neurons in the rat in vivo. *Journal of Comparative Neurology*, *512*(2), 141–157. https://doi.org/10.1002/cne.21879

Jenkinson, M. (2003). Fast, automated, N-dimensional phase-unwrapping algorithm. *Magnetic*

Resonance in Medicine, *49*(1), 193–197. https://doi.org/10.1002/mrm.10354

Jenkinson, M., Beckmann, C. F., Behrens, T. E. J., Woolrich, M. W., & Smith, S. M. (2012). FSL. *NeuroImage*, *62*(2), 782–790. https://doi.org/10.1016/j.neuroimage.2011.09.015

Jenkinson, M., & Smith, S. (2001). A global optimisation method for robust affine registration of brain images. *Medical Image Analysis*, *5*(2), 143–156. Retrieved from http://www.ncbi.nlm.nih.gov/pubmed/11516708

Jones, S. L., & Gebhart, G. F. (1986). Quantitative characterization of ceruleospinal inhibition of nociceptive transmission in the rat. *Journal of Neurophysiology*, *56*(5), 1397–1410. https://doi.org/10.1152/jn.1986.56.5.1397

Kahan, J., Urner, M., Moran, R., Flandin, G., Marreiros, A., Mancini, L., … Foltynie, T. (2014). Resting state functional MRI in Parkinson's disease: The impact of deep brain stimulation on "effective" connectivity. *Brain*, *137*(4), 1130–1144. https://doi.org/10.1093/brain/awu027

Keay, K. A., Feil, K., Gordon, B. D., Herbert, H., & Bandler, R. (1997). Spinal afferents to functionally distinct periaqueductal gray columns in the rat: An anterograde and retrograde tracing study. *Journal of Comparative Neurology*, *385*(2), 207–229. https://doi.org/10.1002/(SICI)1096-9861(19970825)385:2<207::AID-CNE3>3.0.CO;2-5

Kerns, J. G. (2006). Anterior cingulate and prefrontal cortex activity in an FMRI study of trial-to-trial adjustments on the Simon task. *NeuroImage*, *33*(1), 399–405. https://doi.org/10.1016/j.neuroimage.2006.06.012

Kim, C., Kroger, J. K., & Kim, J. (2011). A functional dissociation of conflict processing within anterior cingulate cortex. *Human Brain Mapping*, *32*(2), 304–312. https://doi.org/10.1002/hbm.21020

Kucyi, A., Salomons, T. V, & Davis, K. D. (2013). Mind wandering away from pain dynamically engages antinociceptive and default mode brain networks. *Proceedings of the National Academy of Sciences of the United States of America*, *110*(46), 18692–18697. https://doi.org/10.1073/pnas.1312902110

Lau, B. K., & Vaughan, C. W. (2014). Descending modulation of pain: The GABA disinhibition hypothesis of analgesia. *Current Opinion in Neurobiology*, *29*, 159–164. https://doi.org/10.1016/j.conb.2014.07.010

Legrain, V., Damme, S. Van, Eccleston, C., Davis, K. D., Seminowicz, D. A., & Crombez, G. (2009). A neurocognitive model of attention to pain: Behavioral and neuroimaging evidence. *Pain*. https://doi.org/10.1016/j.pain.2009.03.020

Lieberman, M. D., & Eisenberger, N. I. (2015). The dorsal anterior cingulate cortex is selective for pain: Results from large-scale reverse inference. *Proceedings of the National Academy of Sciences of the United States of America*, *112*(49), 15250–15255. https://doi.org/10.1073/pnas.1515083112

Linnman, C., Moulton, E. A., Barmettler, G., Becerra, L., & Borsook, D. (2012). Neuroimaging of the periaqueductal gray: state of the field. *NeuroImage*, *60*(1), 505–522. https://doi.org/10.1016/j.neuroimage.2011.11.095

Liu, K. Y., Marijatta, F., Hämmerer, D., Acosta-Cabronero, J., Düzel, E., & Howard, R. J. (2017). Magnetic resonance imaging of the human locus coeruleus: A systematic review. *Neuroscience & Biobehavioral Reviews*, *83*, 325–355. https://doi.org/10.1016/J.NEUBIOREV.2017.10.023

Llorca-Torralba, M., Borges, G., Neto, F., Mico, J. A., & Berrocoso, E. (2016). Noradrenergic Locus Coeruleus pathways in pain modulation. *Neuroscience*, *338*, 93–113. https://doi.org/10.1016/j.neuroscience.2016.05.057

Lorenz, J., Minoshima, S., & Casey, K. L. (2003). Keeping pain out of mind: The role of the dorsolateral prefrontal cortex in pain modulation. *Brain*, *126*(5), 1079–1091. https://doi.org/10.1093/brain/awg102

Ma, L., Steinberg, J. L., Cunningham, K. A., Lane, S. D., Kramer, L. A., Narayana, P. A., … Moeller, F. G. (2015). Inhibitory behavioral control: A stochastic dynamic causal modeling study using network discovery analysis. *Brain Connectivity*, *5*(3), 177–186. https://doi.org/10.1089/brain.2014.0275

Ma, L., Steinberg, J. L., Hasan, K. M., Narayana, P. A., Kramer, L. A., & Moeller, F. G. (2014). Stochastic dynamic causal modeling of working memory connections in cocaine dependence. *Human Brain Mapping*, *35*(3), 760–778. https://doi.org/10.1002/hbm.22212

Manella, L. C., Petersen, N., & Linster, C. (2017). Stimulation of the locus ceruleus modulates signal-to-noise ratio in the olfactory bulb. *Journal of Neuroscience*, *37*(48), 11605–11615. https://doi.org/10.1523/JNEUROSCI.2026-17.2017

McLaren, D. G., Ries, M. L., Xu, G., & Johnson, S. C. (2012). A generalized form of context-dependent psychophysiological interactions (gPPI): A comparison to standard approaches. *NeuroImage*, *61*(4), 1277–1286. https://doi.org/10.1016/j.neuroimage.2012.03.068

Millan, M. J. (2002). Descending control of pain. *Progress in Neurobiology*, *66*(6), 355–474. https://doi.org/10.1016/S0301-0082(02)00009-6

Muller, T. H., Mars, R. B., Behrens, T. E., & O'Reilly, J. X. (2019). Control of entropy in neural models of environmental state. *ELife*, *8*. https://doi.org/10.7554/eLife.39404

Nichols, T. E., & Holmes, A. P. (2002). Nonparametric permutation tests for functional neuroimaging: a primer with examples. *Human Brain Mapping*, *15*(1), 1–25. Retrieved from http://www.ncbi.nlm.nih.gov/pubmed/11747097

O'Reilly, J. X., Woolrich, M. W., Behrens, T. E. J., Smith, S. M., & Johansen-Berg, H. (2012). Tools of the trade: Psychophysiological interactions and functional connectivity. *Social Cognitive and Affective Neuroscience*, *7*(5), 604–609. https://doi.org/10.1093/scan/nss055

Oldfield, R. C. (1971). The assessment and analysis of handedness: the Edinburgh inventory. *Neuropsychologia*, *9*(1), 97–113. Retrieved from http://www.ncbi.nlm.nih.gov/pubmed/5146491

Osório, P., Rosa, P., Silvestre, C., & Figueiredo, P. (2015). Stochastic dynamic causal modelling of fMRI data with multiple-model kalman filters. *Methods of Information in Medicine*, *54*(3), 232–239. https://doi.org/10.3414/ME13-02-0052

Ossipov, M. H., Dussor, G. O., & Porreca, F. (2010). Central modulation of pain. *The Journal of*

Clinical Investigation, *120*(11), 3779–3787. https://doi.org/10.1172/JCI43766

Penny, W. D., Stephan, K. E., Daunizeau, J., Rosa, M. J., Friston, K. J., Schofield, T. M., & Leff, A. P. (2010). Comparing Families of Dynamic Causal Models. *PLoS Computational Biology*, *6*(3), e1000709. https://doi.org/10.1371/journal.pcbi.1000709

Petrovic, P. (2002). Placebo and Opioid Analgesia-- Imaging a Shared Neuronal Network. *Science*, *295*(5560), 1737–1740. https://doi.org/10.1126/science.1067176

Petrovic, P., Petersson, K. M., Ghatan, P. H., Stone-Elander, S., & Ingvar, M. (2000). Pain-related cerebral activation is altered by a distracting cognitive task. *Pain*, *85*(1–2), 19–30. https://doi.org/10.1016/S0304-3959(99)00232-8

Peyron, R., Laurent, B., & García-Larrea, L. (2000). Functional imaging of brain responses to pain. A review and meta-analysis (2000). *Neurophysiologie Clinique/Clinical Neurophysiology*, *30*(5), 263–288. https://doi.org/10.1016/S0987-7053(00)00227-6

Potter, M. C., & Levy, E. I. (1969). Recognition memory for a rapid sequence of pictures. *Journal of Experimental Psychology*, *81*(1), 10–15. Retrieved from http://www.ncbi.nlm.nih.gov/pubmed/5812164

Quintero, G. C. (2013). Advances in cortical modulation of pain. *Journal of Pain Research*, *6*, 713–725. https://doi.org/10.2147/JPR.S45958

Rainville, P., Duncan, G. H., Price, D. D., Carrier, B., & Bushnell, M. C. (1997). Pain affect encoded in human anterior cingulate but not somatosensory cortex. *Science*, *277*(5328), 968–971. https://doi.org/10.1126/science.277.5328.968

Ramos, B. P., & Arnsten, A. F. T. (2007). Adrenergic pharmacology and cognition: focus on the prefrontal cortex. *Pharmacol Ther*, *113*(3), 523–536. https://doi.org/10.1016/j.pharmthera.2006.11.006

Ray, S., Di, X., & Biswal, B. B. (2016). Effective connectivity within the mesocorticolimbic system during resting-state in cocaine users. *Frontiers in Human Neuroscience*, *10*(NOV2016). https://doi.org/10.3389/fnhum.2016.00563

Rigoux, L., Stephan, K. E., Friston, K. J., & Daunizeau, J. (2014). Bayesian model selection for group studies — Revisited. *NeuroImage*, *84*, 971–985. https://doi.org/10.1016/J.NEUROIMAGE.2013.08.065

Roelofs, J., Peters, M. L., Zeegers, M. P. A., & Vlaeyen, J. W. S. (2002). The modified Stroop paradigm as a measure of selective attention towards pain-related stimuli among chronic pain patients: a meta-analysis. *European Journal of Pain*, *6*(4), 273–281. https://doi.org/10.1053/eujp.2002.0337

Roy, M., Shohamy, D., Daw, N., Jepma, M., Wimmer, G. E., & Wager, T. D. (2014). Representation of aversive prediction errors in the human periaqueductal gray. *Nature Neuroscience*, *17*(11), 1607–1612. https://doi.org/10.1038/nn.3832

Sales, A. C., Friston, K. J., Jones, M. W., Pickering, A. E., & Moran, R. J. (2019). Locus Coeruleus tracking of prediction errors optimises cognitive flexibility: An Active Inference model. *PLoS Computational Biology*, *15*(1). https://doi.org/10.1371/journal.pcbi.1006267

Sara, S. J. (1985). The locus coeruleus and cognitive function: Attempts to relate nor adrenergic enhancement of signal/noise in the brain to behavior. In *Physiological Psychology* (Vol. 13).

Sara, S. J. (2009). The locus coeruleus and noradrenergic modulation of cognition. *Nat Rev Neurosci*, *10*(3), 211–223. https://doi.org/10.1038/nrn2573

Sara, S. J., & Bouret, S. (2012). Orienting and Reorienting: The Locus Coeruleus Mediates Cognition through Arousal. *Neuron*, *76*(1), 130–141. https://doi.org/10.1016/J.NEURON.2012.09.011

Scholl, J., Kolling, N., Nelissen, N., Stagg, C. J., Harmer, C. J., & Rushworth, M. F. S. (2017). Excitation and inhibition in anterior cingulate predict use of past experiences. *ELife*, *6*. https://doi.org/10.7554/eLife.20365

Smith, S. M., & Nichols, T. E. (2009). *Threshold-Free Cluster Enhancement: Addressing problems of smoothing, threshold dependence and localisation in cluster inference*. Retrieved from https://www.fmrib.ox.ac.uk/datasets/techrep/tr08ss1/tr08ss1.pdf

Sprenger, C., Eippert, F., Finsterbusch, J., Bingel, U., Rose, M., & Büchel, C. (2012). Attention Modulates Spinal Cord Responses to Pain. *Current Biology*, *22*(11), 1019–1022. https://doi.org/10.1016/J.CUB.2012.04.006

Tracey, I., Ploghaus, A., Gati, J. S., Clare, S., Smith, S., Menon, R. S., & Matthews, P. M. (2002). Imaging attentional modulation of pain in the periaqueductal gray in humans. *The Journal of Neuroscience : The Official Journal of the Society for Neuroscience*, *22*(7), 2748–2752. https://doi.org/20026238

Valet, M., Sprenger, T., Boecker, H., Willoch, F., Rummeny, E., Conrad, B., … Tolle, T. R. (2004). Distraction modulates connectivity of the cingulo-frontal cortex and the midbrain during pain - An fMRI analysis. *Pain*, *109*(3), 399–408. https://doi.org/10.1016/j.pain.2004.02.033

van Veen, V., & Carter, C. S. (2005). Separating semantic conflict and response conflict in the Stroop task: A functional MRI study. *NeuroImage*, *27*(3), 497–504. https://doi.org/10.1016/J.NEUROIMAGE.2005.04.042

Vazey, E. M., Moorman, D. E., & Aston-Jones, G. (2018). Phasic locus coeruleus activity regulates cortical encoding of salience information. *Proceedings of the National Academy of Sciences of the United States of America*, *115*(40), E9439–E9448. https://doi.org/10.1073/pnas.1803716115

Wager, T. D., Atlas, L. Y., Botvinick, M. M., Chang, L. J., Coghill, R. C., Davis, K. D., … Yarkoni, T. (2016, May 3). Pain in the ACC? *Proceedings of the National Academy of Sciences of the United States of America*, Vol. 113, pp. E2474–E2475. https://doi.org/10.1073/pnas.1600282113

Wager, T. D., Atlas, L. Y., Lindquist, M. A., Roy, M., Woo, C.-W., & Kross, E. (2013). An fMRI-Based Neurologic Signature of Physical Pain. *New England Journal of Medicine*, *368*(15), 1388–1397. https://doi.org/10.1056/NEJMoa1204471

Wager, T. D., Jonides, J., & Reading, S. (2004). Neuroimaging studies of shifting attention: a meta-analysis. *NeuroImage*, *22*(4), 1679–1693.

https://doi.org/10.1016/J.NEUROIMAGE.2004.03.052

Wittfoth, M., Küstermann, E., Fahle, M., & Herrmann, M. (2008). The influence of response conflict on error processing: Evidence from event-related fMRI. *Brain Research*, *1194*, 118–129. https://doi.org/10.1016/J.BRAINRES.2007.11.067

Woolrich, M. W., Ripley, B. D., Brady, M., & Smith, S. M. (2001). Temporal autocorrelation in univariate linear modeling of FMRI data. *NeuroImage*, *14*(6), 1370–1386. https://doi.org/10.1006/nimg.2001.0931

Yarkoni, T., Poldrack, R. A., Nichols, T. E., Van Essen, D. C., & Wager, T. D. (2011). Large-scale automated synthesis of human functional neuroimaging data. *Nature Methods*, *8*(8), 665–670. https://doi.org/10.1038/nmeth.1635

Yu, A. J., & Dayan, P. (2005). Uncertainty, neuromodulation, and attention. *Neuron*, *46*(4), 681–692. https://doi.org/10.1016/j.neuron.2005.04.026

Zeidan, F., Adler-Neal, A. L., Wells, R. E., Stagnaro, E., May, L. M., Eisenach, J. C., … Coghill, R. C. (2016). Mindfulness-Meditation-Based Pain Relief Is Not Mediated by Endogenous Opioids. *The Journal of Neuroscience : The Official Journal of the Society for Neuroscience*, *36*(11), 3391–3397. https://doi.org/10.1523/JNEUROSCI.4328-15.2016

Zeidan, F., Grant, J. A., Brown, C. A., McHaffie, J. G., & Coghill, R. C. (2012). Mindfulness meditation-related pain relief: evidence for unique brain mechanisms in the regulation of pain. *Neuroscience Letters*, *520*(2), 165–173. https://doi.org/10.1016/j.neulet.2012.03.082

Zeidan, F., & Vago, D. R. (2016). Mindfulness meditation-based pain relief: a mechanistic account. *Annals of the New York Academy of Sciences*, *1373*(1), 114–127. https://doi.org/10.1111/nyas.13153

Zhang, J., Li, B., Gao, J., Shi, H., Wang, X., Jiang, Y., … Yao, S. (2015). Impaired frontal-basal ganglia connectivity in male adolescents with conduct disorder. *PLoS ONE*, *10*(12). https://doi.org/10.1371/journal.pone.0145011